DiaMiR: A MicroRNA (miR-23) Microneedle Patch for Type-2 Diabetes Control

George Cheng

North Carolina School of Science and Mathematics; cheng24g@ncssm.edu

Abstract

422 million adults worldwide have diabetes, and 48% of all juvenile deaths are due to diabetes or diabetes-inflicted diseases; diabetes in low-income families has risen rapidly --- up to 21% worldwide. By combining recent advances in microRNA (miR) technology and applying a novel miR-based LNP loading and microneedle hyaluronic chain-linked drug-infusion method, **DiaMiR** (**Dia**betes **M**icroRNA **i**njected **R**eparation) aims to mitigate the adverse effects of Type-2 Diabetes (T2D) by activating T2D-inhibited signaling pathways. This study provides proof of concept, *in-vitro*, and *in-vivo* data for developing a cost-effective and accessible microRNA (miR) - loaded wearable microneedle patch to control T2D. Scanning electronic microscope (SEM) and fluorescence imaging reveal the conformality of the microneedle patch after miR-23 loading. *In-vitro* tests were conducted to investigate miR-23 effects of AKT insulin pathway, PTEN expression, and glucose output/uptake on the liver (HepG2), adipose (3T3-L1), and skeletal muscle (L6) cell lines. *In-vivo* tests (animal studies) were conducted on T2D mouse; IVIS (In-Vivo Imaging System) was used to determine the degradation profile. Results suggest that miR-23 decreased glucose output in HepG2 liver cells [control vs. miR-23b ($p < 0.0001$; highly significant)], but increased glucose uptake in L6 skeletal muscle cells [control vs. miR-23b ($p < 0.0001$)] and 3T3-L1 fat cells [control vs. miR-23b ($p < 0.0001$)]. DiaMiR microneedle patches were able to significantly lowered blood glucose levels in T2D mouse for 3-4 days as seen in DiaMiR blood glucose mouse experimentation (n = 10) and HbA1C% measurements. Furthermore, DiaMiR showed no toxicity in the treated mouse and did not induce inflammation. Using technologies in bioengineering, biomaterials, and sustained drug delivery, our study offers an innovative solution to control T2D.

1.0 Background

1.1 Diabetes Disease Burden

According to the World Health Organization (WHO), diabetes is a chronic metabolic condition characterized by high blood glucose levels; over time, diabetes may lead to damage to the heart, vasculature, eyes, kidneys, and nerves.[1] Over 90% of diabetes mellitus cases are Type 2 Diabetes mellitus (T2D), a condition marked by tissue insulin resistance and an insensitive insulin secretory response.[2, 3] Progression of the T2D makes insulin secretion impossible to maintain glucose homeostasis, producing hyperglycemia or hypoglycemia in various patients' bloodstreams. In T2D, adipose tissues promote insulin resistance (IR) through 1) inflammatory mechanisms, 2) free fatty acid release, and 3) adipose deregulation.[4, 5] The organ systems involved in T2D development mainly include the pancreas, liver, and skeletal muscles --- however other organs like the kidneys, brain, small intestine, and adipose tissue are also affected.[6] Evolving data suggest that adipokine dysregulation, inflammation, abnormalities in gut microbiota, immune dysregulation, and inflammation may be landmarks between pathophysiological signs of T2D.[7]

Recent epidemiological data show alarming data predicting a worrisome projected future for T2D. According to the International Diabetes Federation (IDF), in 2019, diabetes caused 4.2 million deaths, and 463 million adults aged between 20 and 79 years old were living with diabetes; in fact, diabetes was the underlying cause that resulted in at least $720 billion of health expenditures in 2019. Incidence and prevalence of T2D vary accordingly to geographical region, with more than 80% of patients living in low-to-middle-income countries, which poses additional challenges in effective treatment (considering treatment affordability and convenience). Patients with T2D have a 15% increased

risk of all-cause mortality (mortality because of T2D-inflicted diseases) compared to those without diabetes. Cardiovascular disease (CVD) is the most significant cause of morbidity and mortality associated with T2D.[8] The association of diabetes with increased risk of coronary heart disease hazard ratio (HR), ischemic stroke, and other vascular disease-related deaths has been shown in a previous meta-analysis.[9]

The epidemiology of T2D is affected by genetics and the environment (e.g., ethnicity and family history, obesity/low physical activity, intrinsic pathophysiology). Genetic factors followed by exposure to an environment characterized by sedentary behavior and high-calorie intake will likely result in T2D. Genome-wide association studies have identified common glycemic genetic variants for T2D, but this only accounts for 10% of total trait variance, suggesting that rare variants are essential.[10] People of different ethnic origins may have additional specific phenotypes that increase predisposition to clusters of CVD risk factors, including hypertension, insulin resistance, and dyslipidemia.[11] While the true impact of T2D may be unknown, the implicit damage that T2D may unintentionally cause can lead to complications even after "normalizing" treatment-ridden lives.[12]

1.2 Insulin Resistance Development

Insulin Resistance (IR) refers to a decrease in the metabolic response of insulin-responsive cells to insulin or, at a cellular level, an impaired/lower response to circulating insulin by blood glucose levels. There are three categories of IR or insulin-deficient conditions in T2D: (1) decreased insulin secretion; (2) counter-regulatory hormones or non-hormonal bodies impairing insulin receptors or signaling; and (3) impaired insulin response in target tissues.[13] The ratio of insulin/glucagon plays a significant role in this regulation since it determines the degree of phosphorylation of downstream enzymes in the regulatory signaling pathways; hence, excessive secretion of these hormones may be responsible for inducing IR.[14, 15] 3 critical organs are also extra-sensitive to insulin: skeletal muscle, adipose tissue, and liver; a defective action of insulin in these tissues often precedes the development of systemic IR, thus progressively leading to T2D.

1.3 T2D Pathology Conditions

1.3.1 Skeletal Muscle Pathology in T2D

Skeletal muscle IR is the most critical factor in the development of T2D.[16] Under physiological conditions, insulin stimulates muscle glycogen synthesis by enhancing glucose uptake from plasma. Specifically, insulin may bind to the insulin receptor (INSR) in muscle cells, GLUT4 translocation from intracellular compartments (early endosomes (EE), endosomal recycling compartment (ERC), and trans-Golgi network (TGN)) to the plasma membrane. Therefore, mutations that reduce the expression of GLUT4, as well as any defect in either upstream or downstream signaling pathway, would reduce glucose intake into the muscle resulting in hyperglycemia.[17, 18] The activation of INSR is essential for the action of insulin on glucose metabolism; thus, mutations in any of the main phosphorylation sites can impair INSR tyrosine kinase activity, thereby impairing insulin action on skeletal muscles.[19] Especially in T2D, where a significant cause of decreased glucose uptake is the inability to phosphorylate inhibited pathways, the activation of INSR and related pathways (e.g., p-AKT) may help upregulate insulin production. Moreover, mutations in essential proteins of the downstream signaling pathway, such as insulin receptor substrate-1 (IRS-1) and insulin receptor substrate-2 (IRS-2) or phosphoinositide 3-kinase (PI3K), can also impair insulin action in the muscle.

Besides mutations or defective epigenetic regulation, environmental factors can alter muscle glucose uptake. Physical activity increases blood flow into skeletal muscle cells and enhances glucose utilization.[20] Obesity, associated with chronic inflammation, contributes to IR and T2D. Increasing evidence suggests that because of obesity, increased immune cell infiltration and secretion of pro-inflammatory molecules in intramyocellular and peri-muscular adipose tissue leads to skeletal muscle inflammation, thereby transposing into skeletal muscle IR.[21]

1.3.2 Adipose Tissue Pathology in T2D

Adipose tissue is a dynamic tissue capable of synthesizing a wide range of biologically active compounds that regulate metabolic homeostasis at a cellular level.[22] Insulin acts on adipose tissue in two ways: (1) by stimulating glucose uptake and triglyceride synthesis; and (2) by suppressing triglyceride hydrolysis and inducing the uptake of free-fatty acid (FFA) and glycerol from circulation. After consuming food, GLUT4 allows glucose uptake from the bloodstream into adipocytes, activating glycolysis in which glycerol-3-phosphate (glycerol-3-P) is produced and incorporated into lipogenic pathways. Adipose insulin resistance (Adipose-IR) can lead to impaired suppression of lipolysis, impaired glucose uptake, and enhanced FFA release into plasma, even at high insulin levels.[23] As adipose is a significant contributor to the body's energy store, the lack of adipose storage will lead to increased food intake, vamping the cycle of malnutrition. Among the signaling elements affected by adipose-IR, defective AKT activation impairs GLUT4 translocation to the membrane and promotes the activation of lipolytic enzymes that aggravate hyperglycemia. Adipose-IR is associated with glucose intolerance and elevated release of FFA into plasma that accumulates in other tissue. In the case of the liver, FFA accumulation results in impaired insulin signaling that promotes hepatic gluconeogenesis and impairs the glucose-stimulated insulin response, inducing T2D development.

Furthermore, it has been shown that abnormally increased adipose tissue mass and adipocyte size correlate with pathologic vascularization, hypoxia, fibrosis, and macrophage-mediated inflammation.[19] Constant exposure to abnormally increased adipose tissues may produce impaired proinflammatory molecules, which will not bind to simple nor complex sugars as they did before, further inducing T2D development.

1.3.3 Liver Tissue Pathology in T2D

In the liver, insulin does not only regulate glucose production/utilization but also affects lipid metabolism more broadly. When circulating insulin, glucose levels increase, and the pancreas secretes insulin; insulin binding to liver insulin receptor (INSR) induces autophosphorylation of the receptor. Consequently, insulin receptor substrates (IRSs) are recruited and phosphorylated. IRS activates PI3K, which phosphorylates PIP2, generating PIP3. PIP3 then activates PDK1, which phosphorylates AKT. In addition, AKT is phosphorylated by mTORC2; AKT and mTORC2 are critical pathways for insulin regulation in Type-2 Diabetics. Once AKT is fully activated, it participates in several downstream pathways that regulate multiple metabolic processes, including glycogen synthesis, gluconeogenesis, glycolysis, and lipid synthesis.[24] In physiological states, the combined action of glucagon and insulin allows the precise regulation of hepatic glucose output, which is not present in T2D patients. While glucagon induces hepatic glucose production, insulin acts as a potent inhibitor of glucose production when its concentration in the blood is elevated.[25] The effect of insulin on hepatic glucose production is due to direct and indirect mechanisms. The abnormal production of proinflammatory proteins such as adipocytokines and cytokines, combined with conditions such as oxidative stress, can lead to an inflammatory state responsible for altered insulin response by the liver.[26]

1.3.4 Glucose Uptake & Output Summary

Based on previous literature and preliminary experiments (as summarized in **Figure 1**), HepG2 cells (as a model for liver cells) are responsible for glucose output, and T2D 3T3-L1 cells (as a model for fat cells) and T2D L6 cells (as a model for skeletal cells) are responsible for glucose uptake. Through multiple experiments yielding conclusive results, it is also commonly understood that miR-23 decreases HepG2 output and increases 3T3-L1 and L6 uptake, leading to lower blood glucose concentration in T2D-afflicted patients.

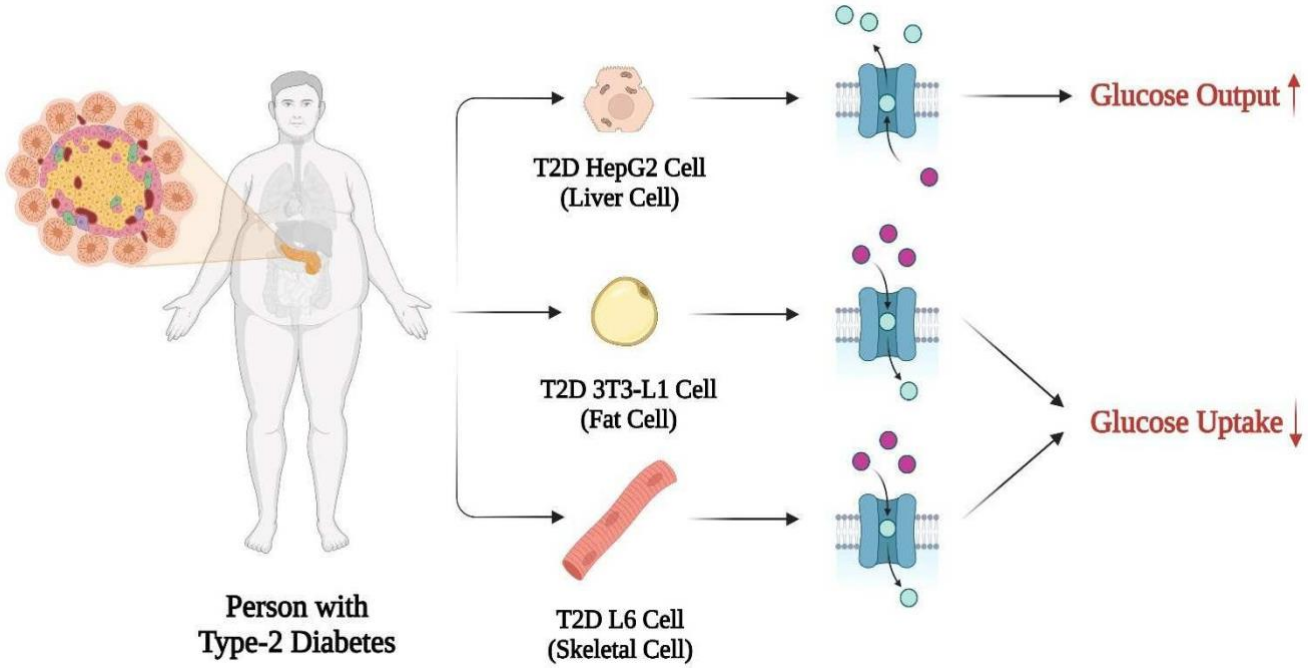

Figure 1: Summarizing glucose output and uptake with corresponding cell lines used in this study.

1.4 MicroRNA and T2D

MicroRNAs (miRNAs or miRs) are a family of endogenous small noncoding RNAs of roughly 22 nucleotides in length; microRNAs bind to the 3′ untranslated regions (UTR) of target genes and inhibit gene expression by degrading and preventing translation of their target messenger RNAs.[27] miRNAs also momentously contribute to organ formation during embryogenesis, including pancreas development and β-cell differentiation.[32] Moreover, they display an essential role in maintaining functional β-cell mass and endocrine cell identity during adult life, which help regulate diabetes-inhibited pathways.[28, 29, 30] Specifically, miR-23b, as established by multiple literature reviews and experimentation, is a prominent inhibitor for inflammation ad cancer STEM cells, specifically through the PTEN/PI3K/AKT pathway.[31]

Previous literature has established the affinity of miRNA to be secreted into extracellular fluids and transported into targeting cells via liposome vesicles.[32] Previous literature has also established correlating levels of miRNA-23 (miR-23) concentration in T2D patients and healthy individuals, establishing the need to validate previous experimentation with miR-23 serum testing in human and mouse models.[24, 25] Literature also validated miR-23 serum concentration correlation with certain cancers, metabolic syndromes, cardiovascular diseases, and other chronic diseases.[33, 34, 35] **Specifically, miR-23 serum concentration has a potential correlation with T2D: miR-23 was significantly lower in T2D patients.** [36, 37] These literature suggests the potential therapeutic role of miR-23 for T2D .

1.5 Microneedle Loading and Delivery

Microneedle patches have been realized as a powerful approach for transdermal drug delivery. They are easy to apply (self-administered), minimally invasive (almost painless), and can achieve long-term sustained drug release. Crosslinked microneedles (containing hyaluronic acid particulates) have been investigated for their degradation abilities and anti-swelling after transdermal drug delivery. Key advantages of using microneedles consist of particulate consistencies in degradation factors and the size of microneedle length (250-500 μm). Further, previous literature cited no decrease in the penetration successrate for crosslinked microneedles (in that the particulate content did not change the dissolution time).[38, 39] Another study captured the biocompatibility, the processability of micro molding, sustained drug release, successful penetration into the skin, and relatively short insertion time for complete disintegration of crosslinked microneedles in the skin.[40] The characteristic features of microneedles are the faster onset of delivery, better patient compliance, self-administration ability, and improved permeability and efficacy.[41] While conventional gold standards (e.g., chemical, lipid enhancers) create nanosized pores (10-20% of alldrug cargo), and hypodermic needles (e.g., hypodermic patches) create deep, pain-receptor-felt pores (30-40% of all drug cargo), drug delivery by minimally-invasive crosslinked microneedles can deliver 90- 100% of the loaded drug.[42, 43]

1.6 Current Diabetes Solutions and Limitations

There are 2 main methods to control the progression of T2D: oral drugs and insulin injections. While insulin injects are fast-acting and provide a continuous injection of insulin, limitations include increased risk of hyperglycemia/hypoglycemia, inconvenience, and cost-effectiveness.[44, 45, 46] Oral drugs, on the other hand, provide inconveniences with delivery time --- combined with potential side-effects associated withenzymatic degradation.[47, 48] DiaMiR aims to eliminate these inconveniences through minimally invasive microneedles and continuous degradation, providing a sustained miR-23 delivery system to combat T2D.

2.0 Methodology

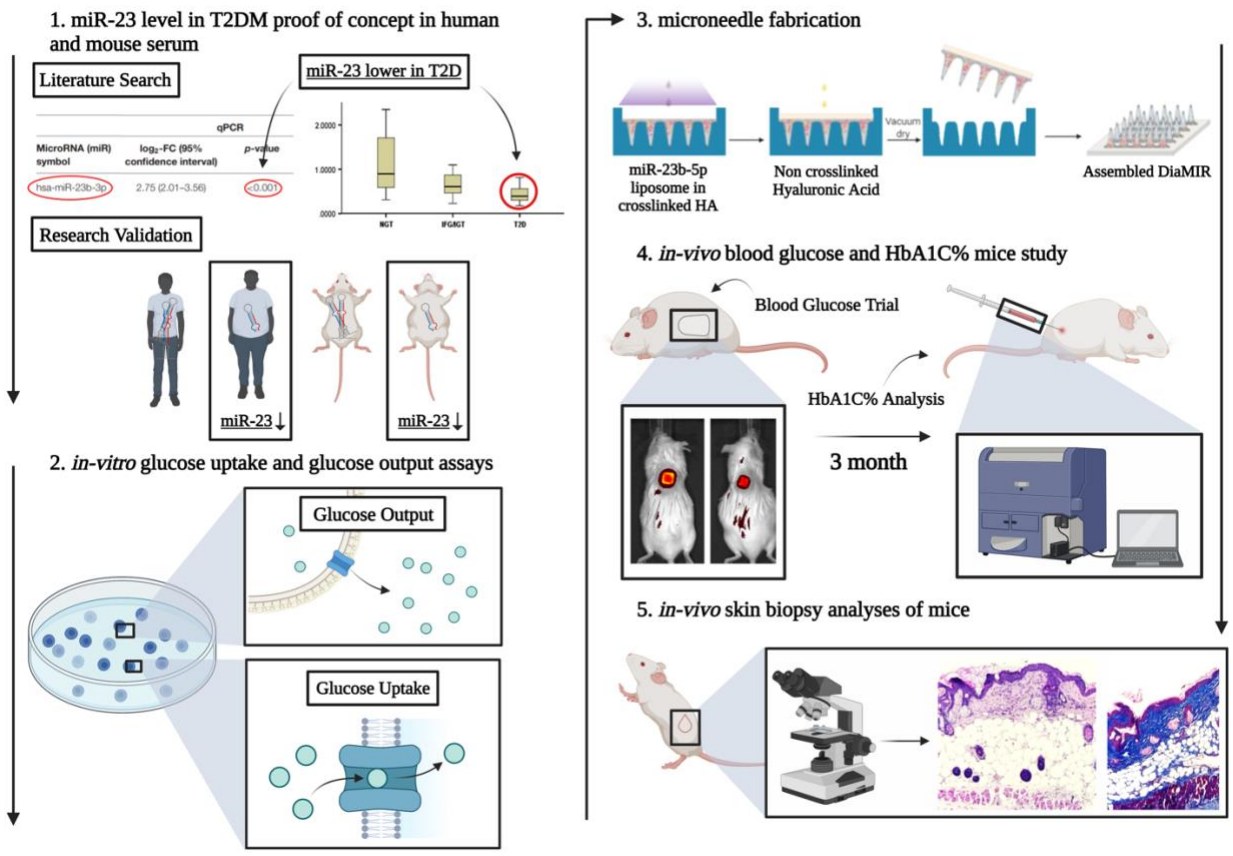

Figure 2: Methodology for DiaMiR consisting of **1)** measuring mir-23 as a proof of concept in human and mouse serum **2)** *in-vitro* glucose uptake/output **3)** microneedle fabrication **4)** *in-vivo* glucose experimentation **5)**and histological analyses of mouse skin biopsy.

2.1 Methodology Overview

Figure 2 details DiaMiR's research methodologies. Specifically, we first analyzed serum from diabetic human and mouse to validate previous literature on miR-23 levels in the blood. After that, using representative cell lines (HepG2, 3T3-L1, and L6), *in-vitro* studies were conducted to evaluate the effects of miR-23 on glucose output and glucose uptake in those aforementioned cell lines. After that, DiaMiR was constructed using crosslinked-microneedle models and loading techniques for miR-23 synthetic mimics. All animal studies were approved by the Institutional Animal Care and Usage Committee (IACUC) at North Carolina State University (Lab Director: Professor Kevin Huang). Mouse studies were performed on transgenic T2D mouse. We applied DiaMiR microneedle patches in those mouse and change for every 3-4 days. Blood glucose levels and HbA1C% were determined. Furthermore, blood chemistry and histology on skin biopsies were performed to ensure safety of the DiaMiR approach.

2.2 Western Blot Analysis

Cells were pretreated with 0.5mM palmitic acid or PBS for 24h and then transfected with has-miR-23 mimic or control mimic for 36h. Before sample collection, cells were treated with 100nM insulin or PBS for 30 mins, and then the cells were homogenized in RIPA buffer supplemented with protease and

phosphatase inhibitors (ThermoFisher Scientific). Whole-cell lysates were collected and quantified using the BCA Protein Assay Kit (Thermo Scientific, USA) and mixed with 4× Laemmli Sample buffer (Bio-Rad, USA). Equal amounts of protein were loaded and resolved on 4–20% SDS polyacrylamide gels, then transferred onto PVDF membranes (Millipore, USA). Next, the membranes were blocked with Tris-buffered saline (TBS) in 5% non-fat milk containing 1% Tween 20 for 1 h at room temperature and then incubated with their corresponding primary antibodies overnight at 4 °C. Membranes were washed with TBS containing 0.1% Tween 20 and then incubated with their corresponding HRP-linked secondary antibodies for 1 h at room temperature. After washing, proteins were visualized using Clarity Western ECL Substrate (Bio-Rad, USA), and images were captured using the ChemiDoc imaging system (Bio-Rad, USA).

2.3 Real-time qPCR

According to the manufacturer's instructions, total RNA was isolated from cells using RNA extraction kits (QIAGEN, Netherlands). cDNA was prepared using iScript™ cDNA Synthesis Kit (Bio-Rad, USA) and qPCR samples were prepared using SsoAdvanced™ Universal SYBR® Green Supermix (Bio-Rad, USA). The qPCR reactions were performed and analyzed using qTOWER^{3}G (Analytikjena, Germany). Relative expression was measured using the ΔΔCT method.

Primers used for qPCR are as follows: G6P-F: GCTTCGCCATCGGATTTTAT, G6P-R: CACCACCTCTGGGCTTTCT, PEPCK-F: GCAAGATTATCGTCACCC, PEPCK-R: GGCATTGAACGCTTTCTCAAAAT, PTEN-F: TGGATTCGACTTAGACTTGACCT, PTEN-R: GGTGGGTTATGGTCTTCAAAAGG, Pten-F: TGAGTTCCCTCAGCCATTGCCT, Pten-R: GAGGTTTCCTCTGGTCCTGGTA.

2.4 Glucose Assays

2.4.1 Glucose Uptake Assay

Glucose uptake in L6 cells and 3T3-L1 cells was analyzed by the 2-NBDG (2-(N-(7- Nitrobenz-2-oxa-1,3-diazol-4-yl)Amino)-2-Deoxyglucose) method (Life Technologies, USA). The differentiated L6 cells and 3T3-L1 cells seeded in 6-well plates were starved for 12 h and transfected with miR-23 in a serum-free medium for 24 h. The medium was discarded, and the cells were washed with PBS three times. Insulin (100 nM) was used to verify the effect of miR-23 inregulating insulin sensitivity (incubated for 30 min). Then, 2-NBDG (100 μM) was added to the cells. After 1h, the cells were collected and subjected to flow cytometric analysis (LSRII, BD).

2.4.2 Measurement of Glucose Production

Glucose production in cultured cells was measured using a commercially available hexokinase-based glucose production assay kit (Abcam). After 24h of transfection with miR-23, the cells were starved for 12h, then treated with 10 nM of insulin, with 100 μM dbcAMP, or with both 10 nM insulin and 100 μM dbcAMP added in the cell medium for 6 h. 50 μl of the medium was collected and mixed with an equal volume of the reaction mix. 450 nm absorbance was measured 60 min after plating.

2.5 Microneedles

2.5.1 Fabrication and Characterization of Cross-linked Microneedles

Microneedle (MN) patch silicone templates and spring applicator were purchased from Micropoint Technologies Pte Ltd (Singapore). The needles were arranged in a 10*10 array with an 800 μm tip in height. We prepared the MN patch with cross-linked hyaluronic acid (HA) as the matrix and non-cross-linked HA as the base. Methacrylate Hyaluronic Acid Hydrogel Kit (Sigma) and a cross-linked HA matrix were prepared according to the product's manual with modifications. Briefly, lyophilized methacrylate HA power was fully dissolved in water (100 mg/2.5 mL, 4%) at 4 °C overnight. Dissolve the photoinitiated Irgacure in methanol at a concentration of 100 mg/mL and then add it to HA methacrylate at the ratio of 1:100 (1 mg for this study) and mix them thoroughly. Load the matrix onto the microneedle mold surface (250 μL) followed by vacuum condition for 5 min to allow the solution to fill the cavities. The residue solution was collected and deposited again to ensure the matrix loading to the needle tips. Afterward, the mold was placed under a 365 nm UV light crosslinking source for 10 min. Then, 1 mL of non-cross-linked HA was added to the top of the microneedle patch to form the base. The microneedle can be placed in a hood overnight to be air-dried. On day 2, the microneedle patch can take out from the mold. To prepare blank microneedle and miR23b loaded microneedle, methacrylate HA (100 mg) was dissolved in 2.5 ml blank liposome solution, or miR23b liposome solution (0.5 nmol miR-23b mimic) at the beginning. The rest procedures are the same. The morphology of the MNs was characterized by a scanning electron microscope (JEOL JCM-7000). An Echo fluorescence microscope took the fluorescence images of the patch.

2.5.2 Application of microneedle patches on mouse

Glucose-lowering capabilities of miR-23b loaded microneedle patch were evaluated in TALLYHO/JgnJ type 2 diabetes mouse (The Jackson Laboratory, 8 weeks). All animal studies were conducted by the principles and procedures outlined in the Guide for the Care and Use of Laboratory Animals and approved by the Institutional Animal Care and Use Committee (IACUC) of North Carolina State University. Animals were housed under a 12 h light/dark circle, allowed food and water ad libitum, and acclimatized for 2 weeks. The blood glucose was measured from tail vein blood samples (~5 μl) of mouse using a True-Track glucose meter (CVS Health, USA). All mouse were fasted overnight before administration and divided into two random groups (n=6), blank microneedle patch and miR-23b loaded microneedle patch. The back fur of the mouse was trimmed, and a microneedle patch was applied to the skin.

2.6 IVIS Imaging, Blood Testing, and Biopsies

To determine the life of microneedles on mouse, we stained the liposome with membrane dye, DiD(Vybrant™ DiD Cell-Labeling Solution, Thermo Fisher) before the preparation of the microneedle patch.The back skin of mouse was imaged on Day 1 and Day 3 after applying the microneedle patch. Blood samples were collected for a complete blood count and chemistry panel (to check liver and kidney functions). In addition, we performed a skin biopsy to examine the effects of the microneedle patch on inflammation in the skin.

3.0 Results

3.1 miR-23 Literature Validation

To validate miR-23 levels as a disease biomarker, we performed two validation experiments with mouse and human samples. Mouse serum (obtained from North Carolina State University Laboratories for Animal Research [LAR]) [C57BL/6] (n = 6) displayed lower serum miR-23 levels in T2D mouse relative to normal mouse (**Figure 3a**; $p \leq 0.05$). Human serum [purchased from LEE BioSolutions] samples were tested from T2D and Healthy patients (n = 10), which demonstrated that serum miR-23 levels in T2D patients were lower than those in healthy donors (**Figure 3b**; $p \leq 0.01$).

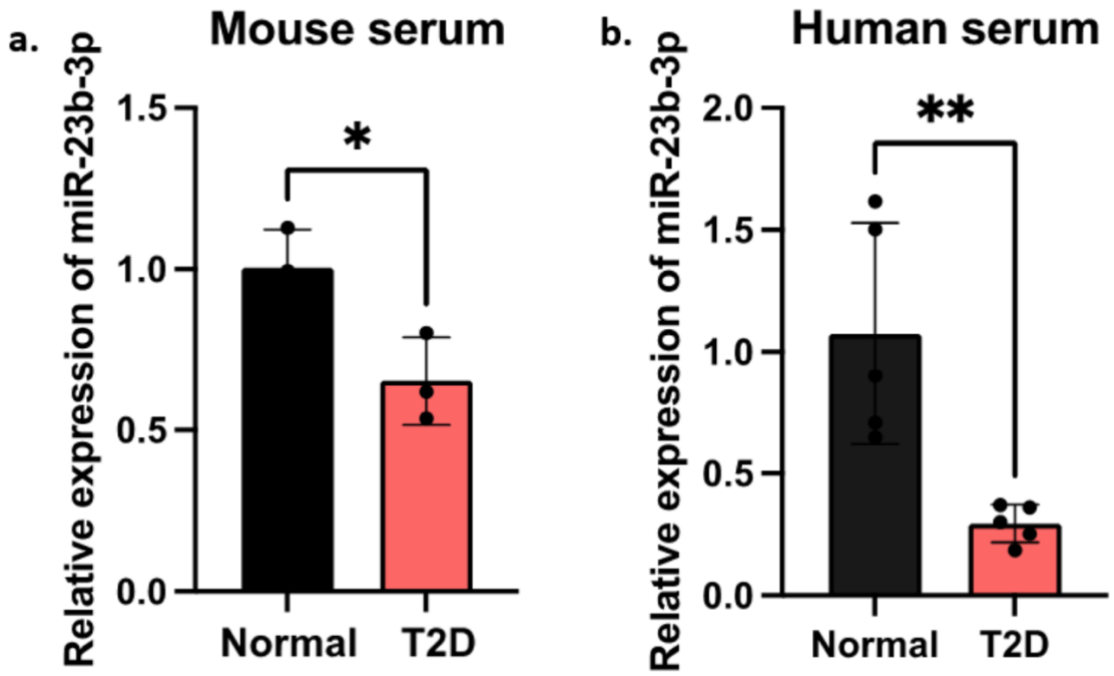

Figure 3: Validation experiment detailing serum miR-23 expressions from **(a)** normal mouse vs. T2D mouse and **(b)** healthy human vs. T2D human. miR-23 levels were measured relative to both Normal mouse and human serum levels, showing a ***significantly*** lower miR-23 expression for T2D mouse & human than normal mouse & human.

* = $p < 0.05$, ** = $p < 0.01$

3.2 Glucose Uptake

Investigating T2D glucose uptake in 2 commonly used cell lines --- namely 3T3-L1 [(adipose cell), ATCC] and L6 [(skeletal muscle cell), ATCC] --- through triplicate assay screening and statistical analyses indiscriminately determined the effects of insulin on T2D and compared both insulin and miR-23 as potential control factors in T2D. Measuring glucose output required fluorescent tracer (2-(N-(7-Nitrobenz-2-oxa-1,3-diazol-4-yl)Amino)-2-Deoxyglucose) (more commonly known as 2-NBDG), a fluorescent analog of glucose that monitors glucose uptake in live cells. Through 2-NBDG positive cells % (or glucose uptake cell percentage), relative comparisons between insulin and miR-23 were derived and analyzed for uptake effectiveness. Furthermore, through 2-NBDG, quantification of percent positive (%) cells was possible (n = 9), which revealed glucose uptake in miR-23 transfected 3T3-L1 cells to be significantly increased compared to the null control ($p \leq 0.0001$) and insulin-only groups ($p \leq 0.001$) **(Figure 4a)**. Specifically, [insulin–, miR-23–] cells were 11.1%, [insulin+, miR-23–] cells were 12.8%, and [insulin+, miR-23+] cells were 23.9% in 3T3-L1 glucose uptake. Quantifying L6 glucose uptake (n = 9) also revealed the same trend regarding miR-23 significance ($p \leq 0.0001$) over null and insulin-only groups **(Figure 4b)**. Specifically, [insulin –, miR-23 –] cells were 14.1%, [insulin +, miR-23 –] cells were 30.2%, and [insulin +, miR-23 +] cells were 45% in 3T3-L1 glucose uptake.

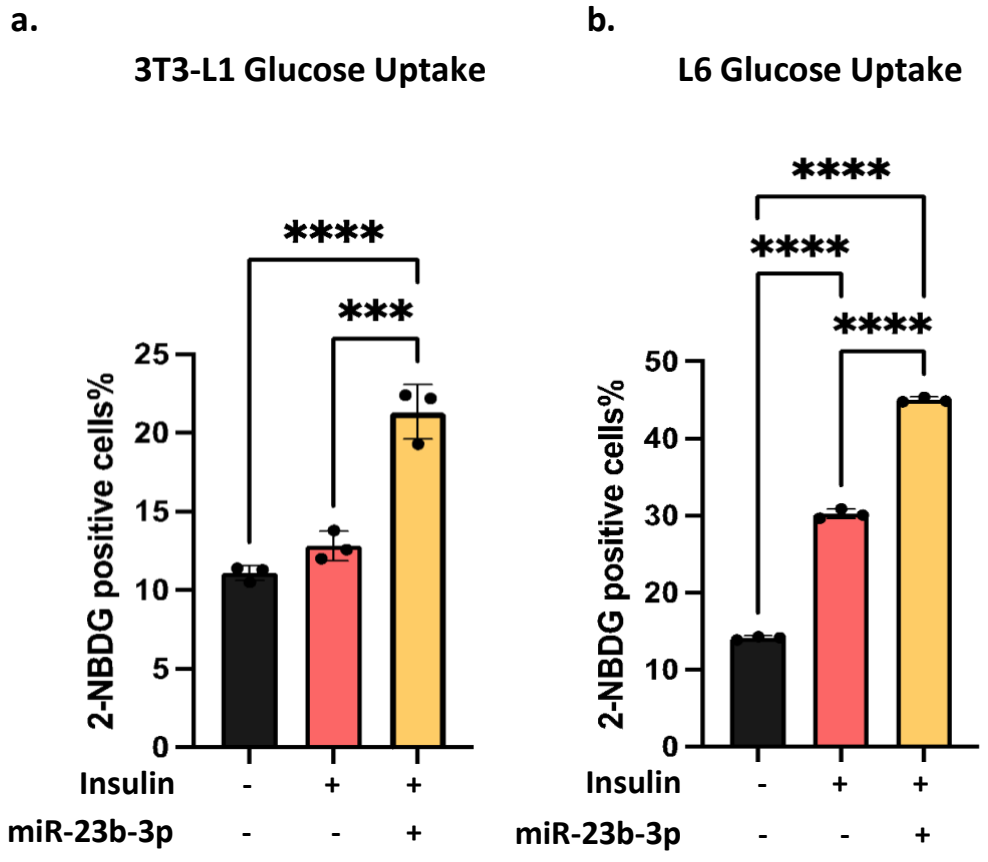

Figure 4: Glucose uptake assay for cell lines 3T3-L1 and L6 through fluorescence tracer 2-NBDG to characterize the effectiveness of miR-23 on glucose uptake. miR-23 treated cells had ***significant*** uptake increase when compared to untreated cells (insulin+, miR-23–) and null cells (insulin–, miR-23–) for both **(a)** 3T3-L1 (adipose) and **(b)** L6 (skeletal) cells lines. *** = $p < 0.001$, **** = $p < 0.0001$

3.3 Glucose Output

Human hepatocellular carcinoma (HepG2) is an immortalized hepatocyte commonly used in diabetes research and toxicity studies [as mentioned in **1.3.3**].[31] Previous studies explored hepatocytes in pathway control system of T2D and found it to be a significant contributor in glucose output.[27, 34, 40] Hepatocytes participate in several downstream pathways regulating multiple metabolic processes, including glycogen synthesis, gluconeogenesis, glycolysis, and lipid synthesis [**1.4.3**]. The HepG2 glucose output assay [HepG2, ATCC] (n = 15) hoped to discover and validate trends in miR-23-induced insulin effectiveness in glucose output compared to insulin with and without the addition of dbcAMP [Sigma]. This phosphodiesterase inhibitor mimicked the action of endogenous cAMP and excited glucose output (to mimic endogenous T2D conditions).

For clarity, each column of glucose output (and its factors) in **Figure 5** was numbered from **1 to 5**. **(1)** [insulin–, dbcAMP–, miR-23–] was the null control, and normalized glucose output measuring at 1.0; **(2)** [insulin+, dbcAMP–, miR-23–] was the insulin-only group measuring at 0.51; and **(3)** [insulin–, dbcAMP+, miR-23–] was the control group that mimics glucose output condition of T2D measuring at 1.97. When compared to **(3)**, the addition of insulin reduced glucose output **(4)** [insulin+, dbcAMP+, miR-23–] as measured in 1.2. However, the addition of miR-23 **(5)** [insulin+, dbcAMP+, miR-23+] produced an even lower glucose output measured at 0.69 --- significant to both **(3)** ($p \leq 0.001$) and **(4)** ($p \leq 0.05$). It is imperative to note that **(2)** only pertains to insulin effects in average glucose output, whereas **(4)** was to T2D-like glucose output.

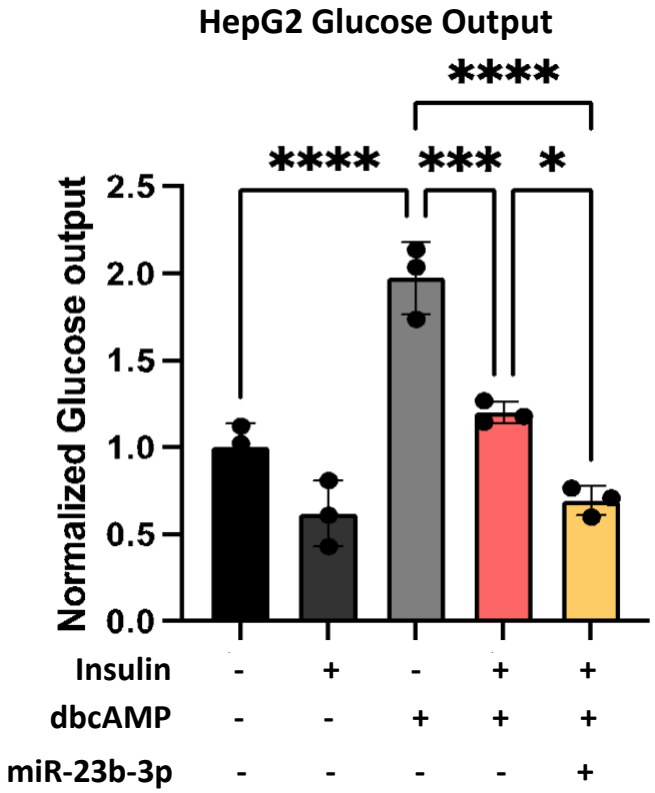

Figure 5: Glucose output assay for cell line HepG2 can be characterized through measuring glucose concentration in media. Whereas insulin inhibits glucose output, dbcAMP mimics the action of endogenous cAMP (a phosphodiesterase inhibitor) and excites glucose output; miR-23 is added to combinations of Insulin and dbcAMP to identify effectiveness; miR-23 ***significantly*** reduced glucose output. * = $p < 0.05$, *** = $p < 0.001$, **** = $p < 0.0001$

3.4 Effects of miR-23 on PTEN Expression

Phosphatase and Tensin Homolog deleted (PTEN), a prominent deregulator of P-AKT (an essential regulator for insulin pathway), is one of the many factors abnormally upregulated by T2D. A significant metabolic role of PTEN is that its altered expression in T2D results in impaired insulin signaling and the promotion of insulin resistance during the pathogenesis of T2D. Loss-of-function PTEN mutations in adipose tissue result in systemic glucose tolerance and insulin sensitivity improvement because of ascended recruitment of the GLUT-4 towards the membrane. Targeting PTEN deletion improves insulin sensitivity and protects from systemic insulin resistance. Hence, miR-23 was tested on two separate tests [mRNA level & protein level) compared to control cells [3T3-L1, ATCC]. **Figure 6a** illustrated miR-23's significant ($p \leq 0.01$) reduction of PTEN expression in mRNA in a triplicate assay; relative expression of PTEN mRNA was normalized to 1.0, and miR-23 PTEN expression was 0.71. **Figure 6b** shows that miR-23+ expression leads to the activation of P-AKT and the inhibition of PTEN.

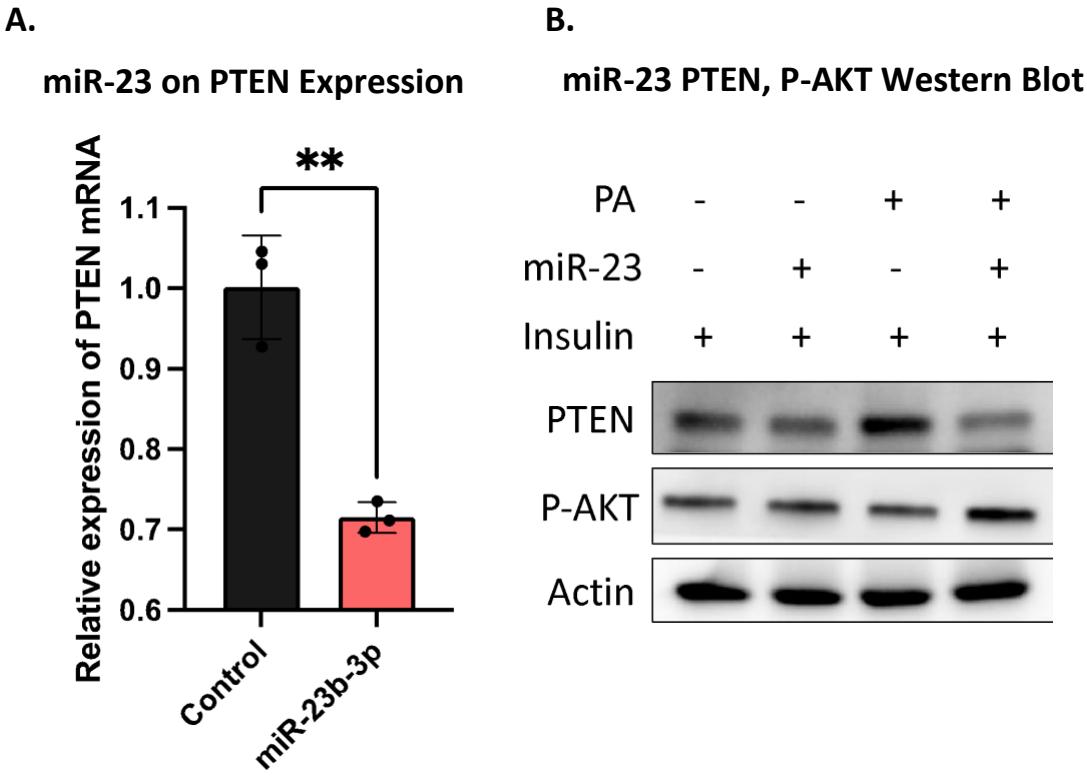

Figure 6: (a) miR-23 ***significantly*** impacts PTEN expression (a prominent deregulator of P-AKT – a necessary pathway for insulin production); **(b)** miR-23 more successfully inhibited PTEN and promoted P-AKT when compared with insulin in western blot analysis. ** = $p < 0.01$

3.5 DiaMiR Microneedle Construction

To construct DiaMiR, as referred to in **Figure 7**, miR-23 mimics was first loaded through a liposome vesicle into hyaluronic acid in a microneedle patch mold. Then, ultraviolet hardening crosslinked the hyaluronic acid with the liposome vesicle-loaded miR-23. Afterward, another layer of hyaluronic acid was poured on the crosslinked and hardened miR-23 layer to act as the base. Finally, after vacuum drying the entire microneedle patch, the DiaMiR base and tip was solidified and combined into one usable product.

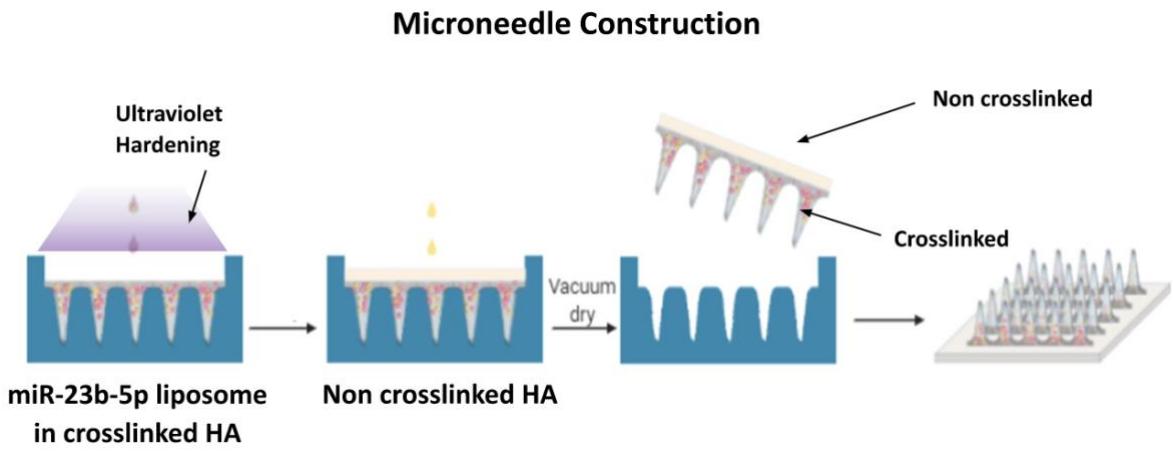

Figure 7: miR-23-loaded microneedles and cross-linkage process. Consisting of **(1)** miR-23 liposome in crosslinked hyaluronic acid (HA) and ultraviolet (UV) hardening; **(2)** this process is then vacuum dried to create a non-crosslinked shell and crosslinked microneedles.

3.6 DiaMiR on HbA1c%

The hemoglobin A1c test, more commonly known as HbA1c%, is a standard diabetes test measuring the amount of hemoglobin A1c (specific hemoglobin chemically linked to monosaccharides and polysaccharides) as an indicator of how well diabetes is controlled. Typically, the lower the HbA1c%, the lower the number of monosaccharides and polysaccharides in the body, thus better control of diabetes in a patient's body.

During experimentation, DiaMiR-treated T2D mouse were subjected to an HbA1c% test comparedto untreated T2D mouse. Subsequently, DiaMiR treatment significantly ($p < 0.05$) reduced the HbA1c% during a triplicate assay conducted between treated and untreated mouse (**Figure 8**). The HbA1c% level forcontrol mouse (untreated) was 7.3% and for miR-23-treated mouse was 5.6%.

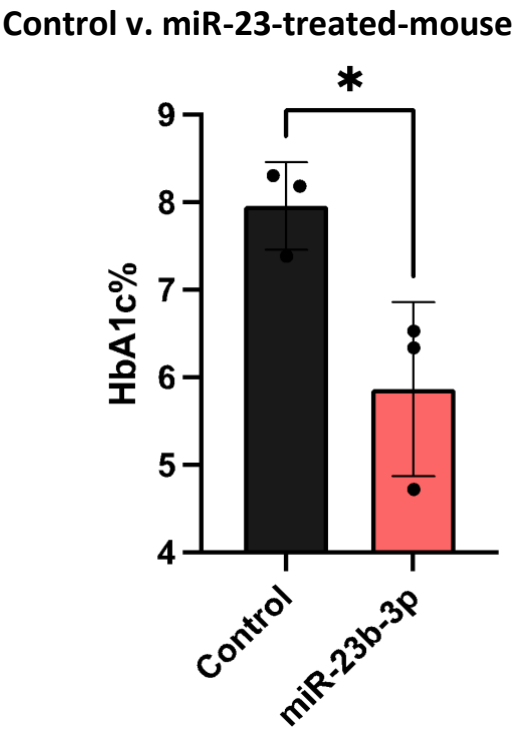

Figure 8: HbA1c% comparison with DiaMiR treated and untreated mouse reveals ***significant*** glucose decrease post experimentation for DiaMiR (miR-23-subjected) treated mouse. * = $p < 0.05$

3.7 DiaMiR on Blood Glucose Levels

All T2D medications and injections aim to reduce the blood glucose flowing in the bloodstream. While earlier sections [as mentioned in **1.1**] discussed the invasiveness of insulin injections or the strenuous delivery of oral drugs, these invasive solutions are proven to reduce blood glucose (backed by previous studies and popular products). Thus, it is imperative for DiaMiR, which has wholly remodeled the invasiveness aspect of T2D control, to achieve the same or significantly better control of blood glucose than the gold standard on the market today; hence, DiaMiR is subjected to both fluorescent staining (**Figure 9a**) and mouse modeling (**Figure 9b**) to discern whether blood glucose is reduced in transgenic T2D mouse.

Figure 9a demonstrated fluorescent imaging for DiaMiR on Day 2 and Day 5 of the T2D mouse model to capture the radiant efficiency (the ratio of the power emitted by a source of radiation to the power consumed by it), essentially measuring whether DiaMiR was still actively releasing miR-23. In a triplicate assay conducted on laboratory mouse (n = 6), DiaMiR remained active after 3 days of miR-23 release and HA disintegration.

Figure 9b investigated the blood glucose differences between DiaMiR-treated and untreated mouse for a 10-day triplicate assay with T2D Mouse (TallyHo/JngJ); n = 10; 5 treated, 5 untreated). Experimentation revealed that after DiaMiR application, there was an immediate significant ($p \leq 0.05$) decrease as seen in **Figure 9b, Day 4:** Untreated Avg. – 512 mg/dL; Treated Avg. – 385 mg/dL and **Figure 9b, Day7:** Untreated Avg. – 531 mg/dL; Treated Avg. – 389 mg/dL. Furthermore, even after the application of DiaMiR, dueto the continuous release of miR-23, blood glucose was controlled significantly lower for up to 2-3 days after application, as seen in **Figure 9b, Day 8:** Untreated – 555 Avg. mg/dL; Treated – 413 Avg. mg/dL.

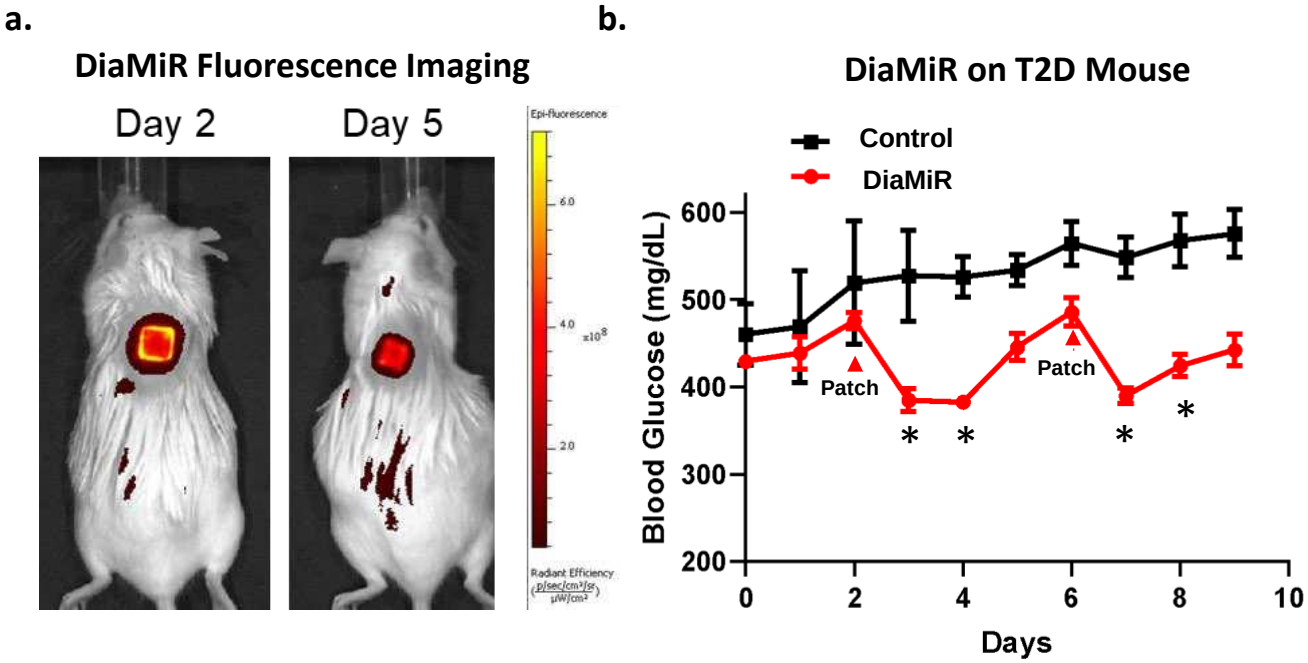

Figure 9: (a) DiaMiR fluorescence imaging for patch contents after 3 days reveals continuous disintegration of microneedle tip and delivery of miR-23 into mouse; **(b)** blood glucose (BG) comparison between DiaMiR treated and untreated mouse in a triplicate assay reveals ***significant*** drops (3) in BG concentration throughout the 10-day experimentation; treated mouse BG concentrations were lower than untreated concentrations ***significantly*** after application. * = $p \leq 0.05$

3.8 Skin Biopsy Analysis to Evaluate Dermal Damage

Analyses of skin biopsies through hematoxylin & eosin staining (H&E staining) and trichome staining allowed for qualitative, visual measurement of the skin after microneedle penetration. Hematoxylin had a deep blue-purple color and stains nucleic acids, whereas eosin is pink and stains proteins nonspecifically. Thus, after DiaMiR penetration, visualization of both potential nucleic acid and protein damage was necessary and indicated no change from pre-experimentation mouse (**Figure 10a**). Trichrome staining was used to visualize connective tissues (mainly collagen) in tissue sections; collagen was stained blue, nuclei were dark brown, muscle tissue was purple, and cytoplasm was pink. Again, no severe visual damage was observed from pre-experimentation mouse, and the dermal layer was not ruptured nor leaking (**Figure 10b**).

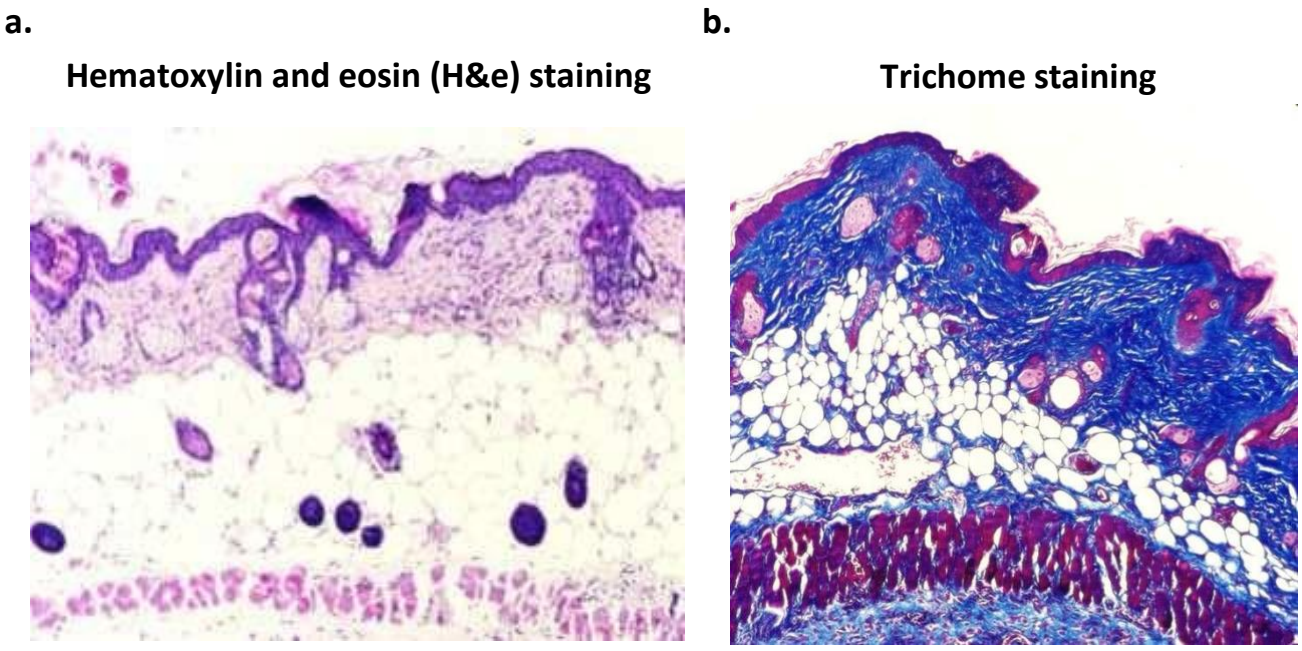

Figure 10: (a) Hematoxylin and eosin (H&e) staining & **(b)** Trichome staining for *in-vivo* histology reveals no severe damage to the dermal layer after applying DiaMiR.

3.9 Blood panel to evaluate toxicity

A blood panel is a laboratory examination of a blood sample used to check for the functioning of specific organs (such as the liver, kidneys, thyroid, and heart) relevant to the study's objective. *Insignificant* results from the blood panel are wanted as they indicate no severe changes compared to the healthy control.

Blood urea nitrogen (BUN) blood test, as seen in **Figure 11a**, measured the amount of urea nitrogen in the blood; elevated levels of BUN can also be due to dehydration, urinary tract obstruction, or congestive heart failure. The normal BUN range is **6 to 34 mg/dL**. The post-experimentation blood panel revealed a 26.3 mg/dL BUN level in control mouse and a 23.3 mg/dL BUN level in miR-23 treated mouse; the blood panel revealed that BUN levels between both groups are *insignificant* ($p > 0.05$).

Alanine transaminase (ALT) blood test, as seen in **Figure 11b**, measured the level of the enzyme ALT in the blood; unusually high levels of ALT in blood concentration can be due to damage or injury to the cells in the liver. The normal ALT range is **24 to 46 IU/L**. The post-experimentation blood panel revealed a 27.6 IU/L ALT level in control mouse and a 29 IU/L ALT level in miR-23 treated mouse; the blood panel revealed ALT levels between both groups are *insignificant* ($p > 0.05$).

Aspartate aminotransferase (AST) blood test, as seen in **Figure 11c**, measured the level of the enzyme ALT in the blood; abnormally high levels of AST in the blood may be a sign of hepatitis, cirrhosis, mononucleosis, or other liver diseases. The normal AST range is **48 to 73 IU/L**. The post-experimentation blood panel revealed a 58 IU/L AST level in control mouse and a 75 IU/L AST level inmiR-23 treated mouse; the blood panel revealed AST levels between both groups are *insignificant* ($p > 0.05$).

Amylase blood test, as seen in **Figure 11d**, measured the amount of enzyme amylase in the urinary tract; uncommon amylase levels indicated pancreatitis or pancreatic damage. The normal amylase range is 1950 to 40 IU/L. The post-experimentation blood panel revealed a 2771 IU/L amylase level in control mouse and a 2689 IU/L amylase level in miR-23 treated mouse; the blood panel revealed that amylase levels between both groups are *insignificant* ($p > 0.05$).

The albumin blood test, as seen in **Figure 11e**, measured the amount of albumin in the blood; high albumin levels indicate potential dehydration or abnormal protein consumption. The normal albumin range is **3.4 to 5.4 g/dL**. The post-experimentation blood panel revealed a 2.8 g/dL albumin level in control mouse and a 2.9 g/dL albumin level in miR-23 treated mouse; the blood panel revealed albumin levels between both groups are *insignificant* ($p > 0.05$).

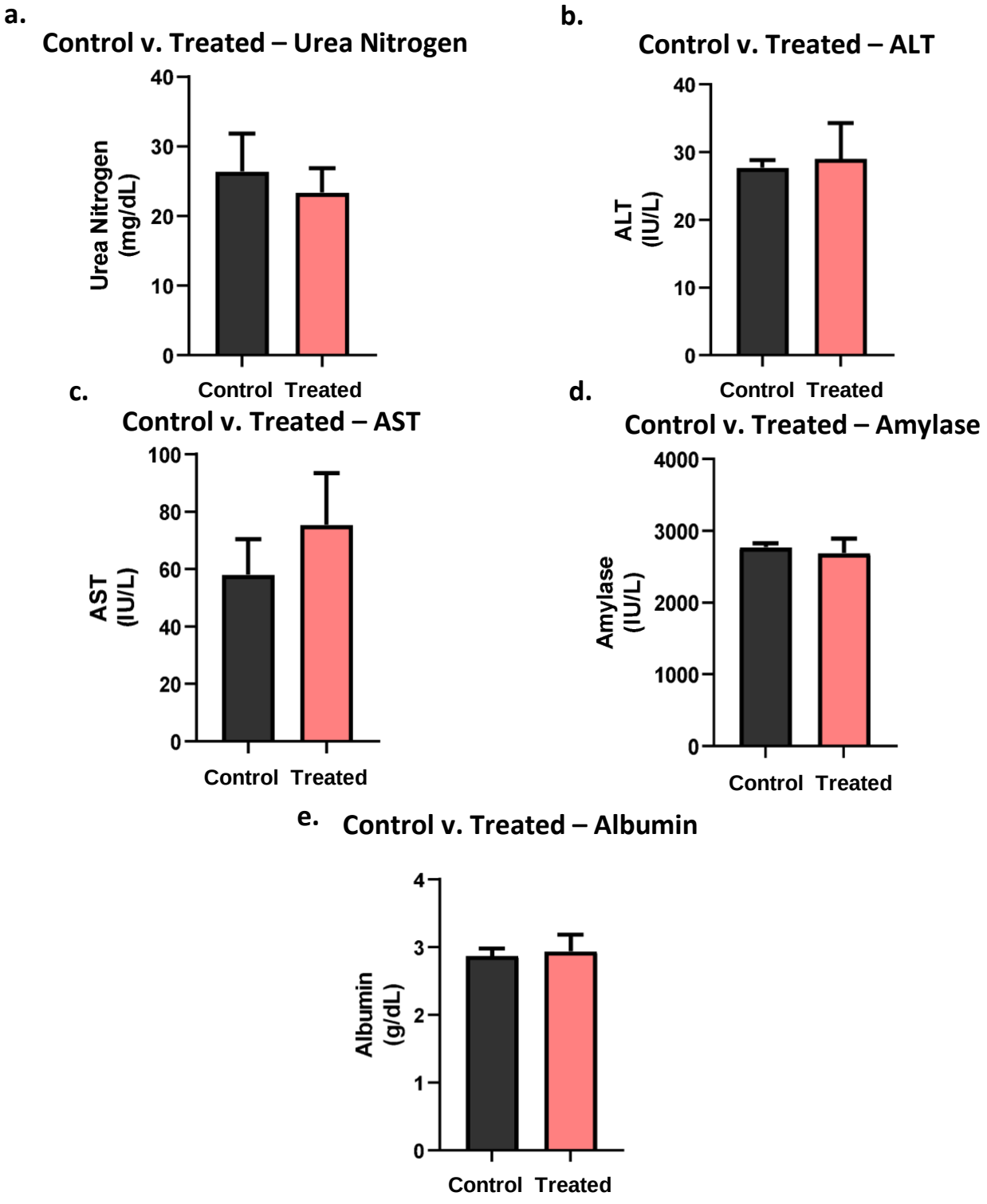

Figure 11: Evaluation of DiaMiR toxicity through **(a)** urea nitrogen, **(b)** ALT, **(c)** AST, **(d)** amylase, and **(e)** albumin between treated and control groups reveals ***insignificant*** ($p > 0.05$) differences between DiaMiR untreated and treated groups.

3.10 Blood routine to evaluate inflammation

A blood routine is a laboratory examination of a blood sample used to check for standard components in blood relevant to the study's objective (e.g., white blood cell, neutrophil). *Insignificant* results from the blood routine are wanted as they indicate no severe changes compared to the healthy control.

White blood cell (WBC) examination, as seen in **Figure 12a**, quantified white blood cells in a microliter of blood; low WBCs indicated a higher susceptibility to inflammation and infection. The normal WBC range is **3.5 to 9.0 × 10^3/μL**. The post-experimentation blood panel revealed a 3.8 x 10^3/μL WBC count in control mouse and a 3.2 x 10^3/μL WBC count in miR-23 treated mouse; the blood panel revealed WBC levels between both groups are *insignificant* ($p > 0.05$).

Neutrophil examination, as seen in **Figure 12b**, measured the number of neutrophils in a microliter of blood; abnormally low neutrophil levels indicated a higher susceptibility to inflammation and infection. The normal neutrophil range is **0.5 to 2.5 × 10^3/μL**. The post-experimentation blood panel revealed a 0.5 x 10^3/μL neutrophil count in control mouse and a 0.7 x 10^3/μL neutrophil count in miR-23 treated mouse; the blood panel revealed that neutrophil levels between both groups are *insignificant* ($p > 0.05$).

Lymphocyte examination, as seen in **Figure 12c**, quantified the number of lymphocytes in a blood microliter; deficient lymphocyte levels, like WBC and Neutrophil, indicated a higher susceptibility to inflammation and infection. The normal lymphocyte range is **1.0 to 4.8 × 10^3/μL**. The post-experimentation blood panel revealed a 2.4 x 10^3/μL lymphocyte count in control mouse and a 2.7 x 10^3/μLlymphocyte count in miR-23 treated mouse; the blood panel revealed lymphocyte levels between both groups are *insignificant* ($p > 0.05$).

Monocyte examination, as seen in **Figure 12d**, measured the number of monocytes in a microliter of blood; uncommonly low levels of monocyte may contribute to monocytopenia and a decrease in WBC count. The normal monocyte range is **0.15 to 0.6 × 10^3/μL**. The post-experimentation blood panel revealed a 0.11 x 10^3/μL monocyte count in control mouse and a 0.14 x 10^3/μL monocyte count in miR-23 treated mouse; the blood panel revealed that monocyte levels between both groups are *insignificant* ($p > 0.05$).

Eosinophil examination, as seen in **Figure 12e**, measured the amount of eosinophil in a microliter of blood; critically low levels of eosinophil increased the short-term risk of heart failure and death. The normal eosinophil range is **0.05 to 0.5 × 10^3/μL**. The post-experimentation blood panel revealed a 0.13 x 10^3/μL eosinophil level in control mouse and a 0.17 x 10^3/μL eosinophil level in miR-23 treated mouse; the blood panel revealed that eosinophil levels between both groups are *insignificant* ($p > 0.05$).

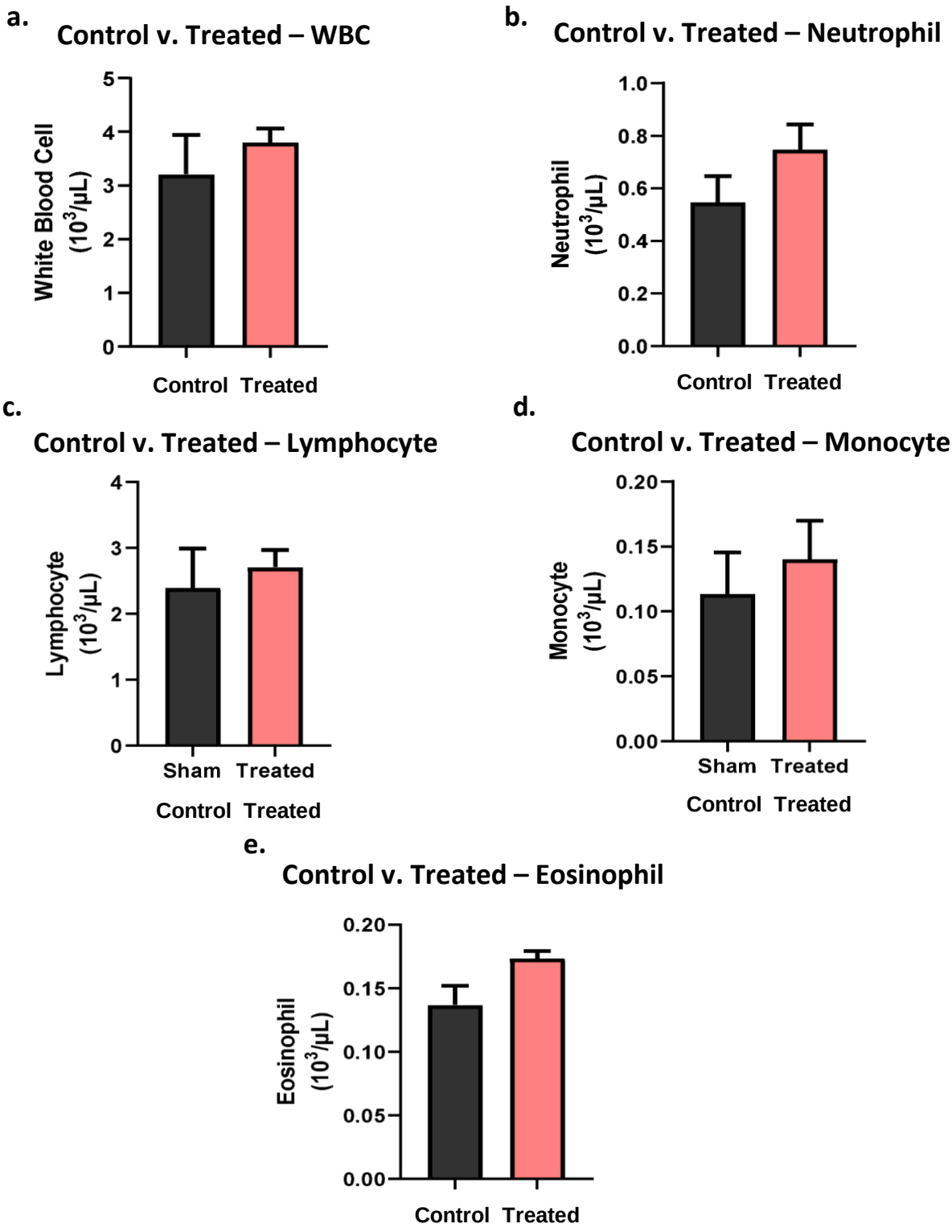

Figure 12: Evaluation of DiaMiR inflammation safety through **(a)** white blood cell count, **(b)** neutrophil, **(c)** lymphocyte, **(d)** monocyte, and **(e)** eosinophil between treated and control groups reveals ***insignificant*** ($p > 0.05$) differences between DiaMiR untreated and treated groups.

4.0 Discussion

4.1 Overview

Type 2 diabetes mellitus (T2D) is a growing worldwide healthcare burden. T2D remains a complicated chronic condition that requires life-long self-monitoring and management. Therefore, studies aiming to improve cost-effectiveness, delivery invasiveness, and develop novel control methods through products like DiaMiR are essential.

4.2 Validation of miR-23 in T2D Human and Mouse Serum

Previous literature reported patterns of miR-23 deficiencies in both T2D human and mouse experimentation, hence testing miR-23 concentration is crucial as the expression of specific pathways (e.g., P-AKT, PI3K) may be inhibited due to T2D. Note that normalization concerning the healthy control was necessary to offer relative significance between healthy and T2D experimental groups. Serum, a fluid and solute component of blood, was readily used for human and mouse experimentations as it contained relevant components like antibodies, antigens, other circulating proteins, salt, and fatty acids. Both mouse and human serum experimentations demonstrated a pattern of miR-23 deficiencies in T2D, which may lead to the under- regulation of beneficial pathways or over-regulation of potentially harmful ones. Significance in both lower expressions of miR-23 validate previous literature findings, thus sparking a possible lead to the hypothesis that increasing miR-23 concentrations in various cell lines may reduce or control T2D expression in both mouse and human models.

4.3 Cell studies

4.3.1 Analyses of Glucose Uptake through miR-23 on L6 (skeletal) and 3T3-L1 (fat) Cell Lines

Glucose uptake is an essential metric to measure as there is a significant difference between glucose uptake for T2D patients and healthy individuals. Increased glucose uptake is optimal as glucose is uptake to be processed and stored rather than continuously flowing in one's bloodstream. As abnormal glucose uptake will lead to an influx of glucose concentration in the bloodstream, it becomes necessary to increase glucose uptake in T2D patients. As both the skeletal and fat cells contribute to the significant uptake of glucose, characterized immortal cell lines myoblast cell L6 was used for skeletal cell characterization, and 3T3-LI cell line was used for adipose/fat cell characterization in *in-vitro* experimentation. Instead of simulating a T2D condition, measuring glucose uptake requires biomarkers (2-(N-(7-Nitrobenz-2-oxa-1,3-diazol-4-yl)Amino)-2-Deoxyglucose), more commonly known as 2-NBDG, to measure and quantify the percentage of cells that absorb this analog between treated and untreated factors, namely: insulin–, miR-23–; insulin+, miR-23–; miR-23+, insulin+. miR-23 significantly increases glucose uptake percentage compared to untreated L6 and 3T3-L1 cell lines by measuring the percentage of 2-NBDG-positive cells. This suggests that increasing miR-23 concentrations in various cell lines may further increase or at least control glucose uptake, thus possibly reducing glucose concentrations in the bloodstream.

4.3.2 Analysis of Glucose Output through miR-23 on HepG2 (liver) Cell Line

Glucose output is an important metric to measure as there is a significant difference between glucose output for T2D patients and healthy individuals. A reduction of glucose output is optimal as glucose is then processed and stored rather than continuously increasing in one's bloodstream. As

abnormal glucose output will lead to an influx of glucose concentration in the bloodstream, it becomes necessary to reduce glucose output in T2D patients. As the liver contributes to the large output of glucose, a characterized immortal cell line hepatoma G2 (HepG2) was used in *in-vitro* experimentation. Further, to mimic conditions of T2D for *in-vitro* studies, a phosphodiesterase inhibitor (dbcAMP) was used to mimic endogenous cAMP, creating a T2D-like environment in HepG2 cells. miR-23 significantly reduces glucose output concentration compared to untreated HepG2 cell lines by measuring the glucose concentration in the secreted media. As quantified, the average glucose production on miR-23 treated T2D-modeled dbcAMP was 0.69, compared to untreated T2D-modeled dbcAMP (1.97); the results were significant. Furthermore, when combined with the T2D-modeled dbcAMP and gold standard insulin 1.2, the average relative glucose production was substantial compared to insulin acting on T2D-modeled dbcAMP (1.97). Note that normalization according to the negative control corresponds to relevant factors cross-sectionally. The purpose of multiple combinations of analyses is to provide insight into insulin v. miR-23 performance, as insulin is the gold standard on the market today. Further, statistical studies between all factors demonstrate the weight of differences from factor to factor (and establish credibility with the data sources found). This suggests that increasing miR-23 concentrations in various cell lines may reduce or control glucose output, thus possibly reducing glucose concentrations in the bloodstream.

4.4 Analyses of DiaMiR effectiveness on Mouse

While previous experimentation was purely based on *in-vitro* data, testing the effectiveness of DiaMiR on mouse models is critical to evaluating the potential for humans. Prior literature conducted proof-of-concept experimentation by measuring miR-23 content in transgenic T2D mouse and healthy control---running multiple blood routines and panels to validate their findings. Further research on miR-23 consisted of literature reviews, miR-23 functionality in mammals, and potential applications of miR-23. This study hopes to expand beyond preliminary research and includes statistics, analyses, and results based on miR-23 effects on T2D mouse.

Epi-fluorescence imaging can heat map and trace the contents of DiaMiR post-injection. DiaMiR is still active after 3 days of degradation, serving as a more resilient, less frequent, and cost-effective method than standard insulin pumps. Blood glucose comparisons between DiaMiR-treated and untreated mouse reveal the first performance testing result for miR-23. Note that mouse have intrinsically higher bloodglucose concentrations, and transgenic mouse can elevate naturally induced T2D by twice the original blood glucose level; hence, transgenic T2D mouse generally start at blood glucose close to 450 mg/dL; since mouse have intrinsically higher blood glucose levels, this experiment also demonstrated the ability ofmir-23 to control blood glucose levels and drastically lower glucose from the bloodstream. Conclusively,DiaMiR is a trustable control method for T2D by significantly lowering blood glucose from the bloodstream in a minimally invasive manner for an extended period.

5.0 Conclusion & Future Directions

DiaMiR (**Dia**betes **M**icroRNA **i**njected **R**eparation) has successfully demonstrated both proofs of concepts (in-vitro) and performance testing (in-vivo) data for developing a cost-effective and accessible miR-23-loaded microneedle patch. Preliminary validation of miR-23 deficiencies in T2D patients was replicated in human and mouse serum studies. Further histological analyses indicate that the toxicity of crosslinked microneedles is negligible (through inflammatory testing and skin biopsy histology). DiaMiR also introduces the concept of microRNA therapy, a relatively underutilized method, through delivery by

minimally invasive means. Western blotting and quantitative Polymerase Chain Reaction (qPCR) testing reveal case-by-case comparisons between individual cell group improvements and general cell line changes. Lastly, the crosslinked hyaluronic microneedles polymerized successfully, and the miR-23 loading process was convenient compared to gold standards. Testing revealed that DiaMiR-treated mouse had significantly lower blood glucose levels than Type-2 Diabetic mouse [control mouse + vs. DiaMiR mouse + ($p \leq 0.01$)]. Furthermore, histology evaluating toxicity between control mouse and DiaMiR mouse was conclusive (controlmouse + vs. DiaMiR mouse +) and relatively similar between both groups. While DiaMiR is a relatively newapproach in incorporating microRNA with a minimally invasive delivery method, bounds for possible usagein humans have been established. Our study covers beyond the preliminary applications of microRNA andcrosslinked microneedles and expands into possible patient care.

6.0 Acknowledgments

Many thanks to Dr. Kevin Huang from North Carolina State University for his contributions to experimentation and data analysis in in-vitro and in-vivo studies. Dr. Zhang from Harvard University – Bioengineering Department for his contribution to microneedle patch conception and minimally invasive injection methodologies. Dr. Cargill from the North Carolina School of Science and Mathematics for mentoring me throughout the scientific process. Lastly, my family for supporting and advising me through the valleys of preliminary testing to the peaks of DiaMiR's success.

7.0 References

1. Roden M., Shulman G. I. “The Integrative Biology of Type 2 Diabetes.” *Nature*, no. 576, pp. 51–60, 2019. doi: 10.1038/s41586-019-1797-8.

2. Stumvoll M., Goldstein B. J., van Haeften T.W. “Type 2 diabetes: Principles of Pathogenesis and Therapy.” *Lancet*, no. 365, pp. 1333-1346, 2005. doi: 10.1016/S0140-6736(05)61032-X.

3. Weyer C., Bogardus C., Mott D. M., Pratley R. E. “The Natural History of Insulin Secretory Dysfunction and Insulin Resistance in the Pathogenesis of Type 2 Diabetes Mellitus.” *J. Clin. Investig.* no. 104, pp. 787-794, 1999. doi: 10.1172/JCI7231.

4. Chatterjee S., Khunti K., Davies M. J. “Type 2 Diabetes.” *Lancet*, no. 389, pp. 2239–2251, 2017. doi: 10.1016/S0140-6736(17)30058-2.

5. “A Pooled Analysis of 751 Population-based Studies with 4.4 Million Participants.” *Lancet*, no. 387, pp. 1513–1530, 2016. doi: 10.1016/S0140-6736(16)00618-8.

6. Defronzo R. A. “From the Triumvirate to the Ominous Octet: A New Paradigm for Treating Type 2 Diabetes Mellitus.” *Diabetes*, no. 58, pp. 773–795, 2009. doi: 10.2337/db09-9028.

7. Schwartz S. S., Epstein S., Corkey B. E., Grant S. F., Gavin J. R., Aguilar R. B. “The Time Is Right for a New Classification System for Diabetes: Rationale and Implications of the beta-Cell-Centric Classification Schema.” *Diabetes Care*, no. 39, pp. 179–186, 2016. doi: 10.2337/dc15-1585.

8. Gaede P., Vedel P., Larsen N., Jensen G. V., Parving H. H., Pedersen O. “Multifactorial Intervention and Cardiovascular Disease in Patients with Type 2 Diabetes.” *N. Engl. J. Med.*, no. 348, pp. 383–393, 2003. doi: 10.1056/NEJMoa021778.

9. Sarwar N., Gao P., Seshasai S. R., Gobin R., Kaptoge S., Di Angelantonio E., Ingelsson E., Lawlor D. A., Selvin E., Stampfer M., *et al.* “Diabetes Mellitus, Fasting Blood Glucose Concentration, and Risk of Vascular Disease: A Collaborative Meta-Analysis of 102 Prospective Studies.” *Lancet*, no. 375, pp. 2215–2222, 2010. doi: 10.1016/S0140-6736(10)60484-9.

10. Grarup N., Sandholt C. H., Hansen T., Pedersen O. “Genetic Susceptibility to Type 2 Diabetes and Obesity: From Genome-Wide Association Studies to Rare Variants and Beyond.” *Diabetologia*, no. 57, pp. 1528–1541, 2014. doi: 10.1007/s00125-014-3270-4.

11. Wong N. D., Zhao Y., Patel R., Patao C., Malik S., Bertoni A. G., Correa A., Folsom A. R., Kachroo S., Mukherjee J., et al. “Cardiovascular Risk Factor Targets and Cardiovascular Disease Event Risk in Diabetes: A Pooling Project of the Atherosclerosis Risk in Communities Study, Multi-Ethnic Study of Atherosclerosis, and Jackson Heart Study.” *Diabetes Care*, no. 39, pp. 668–676, 2016. doi: 10.2337/dc15-2439.

12. Fu Z., Gilbert E. R., Liu D. “Regulation of Insulin Synthesis and Secretion and Pancreatic Beta-cell Dysfunction in Diabetes.” *Curr. Diabetes Rev.*, no. 9, pp. 25–53, 2013. doi: 10.2174/157339913804143225.

13. Liu M., Weiss M. A., Arunagiri A., Yong J., Rege N., Sun J., Haataja L., Kaufman R. J., Arvan P. "Biosynthesis, Structure, and Folding of the Insulin Precursor Protein." *Diabetes Obes. Metab*, no. 20, pp. 28–50, 2018. doi: 10.1111/dom.13378.

14. Dali-Youcef N., Mecili M., Ricci R., Andres E. "Metabolic Inflammation: Connecting Obesity and Insulin Resistance." *Ann. Med.*, no. 45. pp. 242–253, 2013. doi: 10.3109/07853890.2012.705015.

15. Hummasti S., Hotamisligil G. S. "Endoplasmic Reticulum Stress and Inflammation in Obesity and Diabetes." *Circ. Res.*, no. 107, pp. 579–591, 2010. doi: 10.1161/CIRCRESAHA.110.225698.

16. Petersen K. F., Shulman G. I. "Pathogenesis of Skeletal Muscle Insulin Resistance in Type 2 Diabetes Mellitus." *Am. J. Cardiol.*, no. 90, pp. 11–18, 2002. doi: 10.1016/S0002-9149(02)02554-7.

17. Petersen K. F., Shulman G. I. "Cellular Mechanism of Insulin Resistance in Skeletal Muscle." *J. R Soc. Med.*, no. 95, no. 8–13, 2002.

18. Satoh T. "Molecular Mechanisms for the Regulation of Insulin-stimulated Glucose Uptake by Small Guanosine Triphosphatases in Skeletal Muscle and Adipocytes." *Int. J. Mol. Sci.* no. 15, pp. 18677–18692, 2014. doi: 10.3390/ijms151018677.

19. DeFronzo R. A. Lilly. "The Triumvirate: beta-cell, Muscle, Liver. A Collusion Responsible for NIDDM." *Diabetes*, no. 37, pp. 667–687, 1988. doi: 10.2337/diab.37.6.667.

20. Abdul-Ghani M. A., DeFronzo R. A. "Pathogenesis of Insulin Resistance in Skeletal Muscle." *J. Biomed. Biotechnol.*, no. 2010, pp. 4762–4779, 2010. doi: 10.1155/2010/476279.

21. Wu H., Ballantyne C. M. "Skeletal Muscle Inflammation and Insulin Resistance in Obesity." *J. Clin. Investig.*, no. 127, pp. 43–54, 2017. doi: 10.1172/JCI88880.

22. Coelho M., Oliveira T., Fernandes R. "Biochemistry of Adipose Tissue: An Endocrine Organ." *Arch. Med. Sci.*, no. 9, pp. 191–200, 2013. doi: 10.5114/aoms.2013.33181.

23. Rosen E. D., Spiegelman B. M. "Adipocytes as Regulators of Energy Balance and Glucose Homeostasis." *Nature*, no. 444, pp. 847–853, 2006. doi: 10.1038/nature05483.

24. Gastaldelli A., Gaggini M., DeFronzo R. A. "Role of Adipose Tissue Insulin Resistance in the Natural History of Type 2 Diabetes: Results from the San Antonio Metabolism Study." *Diabetes*, no. 2017, pp. 815–822, 2006. doi: 10.2337/db16-1167.

25. Czech M. P. "Mechanisms of Insulin Resistance Related to White, Beige, and Brown Adipocytes." *Mol. Metab*, no. 34, pp. 27–42, 2020. doi: 10.1016/j.molmet.2019.12.014.

26. Scherer P. E. "The Many Secret Lives of Adipocytes: Implications for Diabetes." *Diabetologia*, no. 62, pp. 223–232, 2019. doi: 10.1007/s00125-018-4777-x.

27. Maki K. C., Kelley K. M., Lawless A. L., Hubacher R. L., Schild A. L., Dicklin M. R., Rains T. M. "Validation of Insulin Sensitivity and Secretion Indices Derived from the Liquid Meal Tolerance Test." *Diabetes Technol. Ther*, no. 13, pp. 661–666, 2011. doi: 10.1089/dia.2010.0240.

28. Titchenell P. M., Lazar M. A., Birnbaum M. J. "Unraveling the Regulation of Hepatic Metabolism by Insulin." *Trends Endocrinol. Metab*, no. 28, pp. 497–505, 2017. doi: 10.1016/j.tem.2017.03.003.

29. Cherrington A. D., Moore M. C., Sindelar D. K., Edgerton D. S. “Insulin Action on the Liver *in vivo*. *Biochem. Soc. Trans.*, no. 35, pp. 1171–1174, 2007. doi: 10.1042/BST0351171.

30. Kato M., Zhang J., Wang M., Lanting L., Yuan H., Rossi J. J., *et al.* “Microrna-192 in Diabetic Kidney Glomeruli and its Function in tgf-beta-induced Collagen Expression via Inhibition of E-box Repressors.” *Proc. Natl. Acad. Sci. U. S. A.*, no. 104, pp. 3432-3437, 2007.

31. Kulkarni A. A., Thatcher T. H., Olsen K. C., Maggirwar S. B., Phipps R. P., Sime P. J. “Ppar-gamma Ligands Repress tgf-beta-induced Myofibroblast Differentiation by Targeting the pi3k/Akt Pathway: Implications for Therapy of Fibrosis.” *PloS One*, no. 6, pp. 159-209, 2011.

32. Leone V., D’Angelo D., Pallante P., Croce C. M., Fusco A. “Thyrotropin Regulates Thyroid Cell Proliferation by Up-Regulating mir-23b and mir-29b that Target smad3” *J. Clin. Endocrinol. Metab.*, no. 97, pp. 3292-3301, 2012.

33. Leone V., Langella C., D’Angelo D., Mussnich P., Wierinckx A., Terracciano L., *et al.* “mir-23b and mir-130b Expression is Downregulated in Pituitary Adenomas” *Mol. Cell. Endocrinol.*, no. 390, pp. 1-7, 2014.

34. Li R., Wang Y., Liu Y., Chen Q., Fu W., Wang H., *et al.* “Curcumin Inhibits Transforming Growth factor-beta1-induced EMT via Ppargamma Pathway, not smad Pathway in Renal Tubular Epithelial Cells.” *PloS One*, no. 8, pp. e58848, 2013.

35. Han Z., Zhou X., Li S., Qin Y., Chen Y., Liu H. “Inhibition of miR-23a Increases the Sensitivity of Lung Cancer Stem Cells to Erlotinib through PTEN/PI3K/Akt pathway.” *Oncol Rep*. no. 38, pp. 3064-3070, 2017. doi:10.3892/or.2017.5938.

36. Kim H. K., Lee S. H., Lee B. Y., *et al.* “A Comparative Study of Dissolving Hyaluronic Acid Microneedles with Trehalose and Poly (Vinyl Pyrrolidone) for Efficient Peptide Drug Delivery. *Biomaterials Science*, no. 6, pp. 2566–2570, 2018. doi: 10.1039/c8bm00768c.

37. Larrañeta E., Henry M., Irwin N. J., Trotter J., Perminova A. A., Donnelly R. F. “Synthesis and Characterization of Hyaluronic Acid Hydrogels Crosslinked using a Solvent-free Process for Potential Biomedical Applications.” *Carbohydrate Polymers*, no. 181, pp. 1194-1205, 2018. doi: 10.1016/j.carbpol.2017.12.015.

38. Wang C., Ye Y., Hochu G. M., Sadeghifar H., Gu Z. “Enhanced Cancer Immunotherapy by Microneedle Patch-assisted Delivery of anti-pd1 Antibody.” *Nano Letters*, no. 16, pp. 2334–2340, 2016. doi: 10.1021/acs.nanolett.5b05030.

39. Korkmaz E., Friedrich E. E., Ramadan M. H., et al. “Tip-loaded Dissolvable Microneedle Arrays Effectively Deliver Polymer-Conjugated Antibody Inhibitors of Tumor-Necrosis-Factor-alpha into Human Skin.” *Journal of Pharmaceutical Sciences*, no. 105, pp. 3453-3457, 2016. doi: 10.1016/j.xphs.2016.07.008.

40. Dong L., Li Y., Li Z., *et al.* “Au Nanocage-Strengthened Dissolving Microneedles for Chemo-Photothermal Combined Therapy of Superficial Skin Tumors.” *ACS Applied Materials & Interfaces*, no. 10, pp. 9247-9256, 2018. https://doi.org/10.1021/acsami.7b18293.

41. Kim D. S., Choi J. T., Kim C. B., *et al.* "Microneedle Array Patch (MAP) Consisting of Crosslinked Hyaluronic Acid Nanoparticles for Processability and Sustained Release." *Pharm Res*, no. 37, pp. 50-72, 2020. https://doi.org/10.1007/s11095-020-2768-3.

42. Tejashree W., Gautam S., Sunil K. D., Murali M. P., Gaurav G., Mahaveer S., Kamal D., *et al*. "Microneedles: A Smart Approach and Increasing Potential for Transdermal Drug Delivery System." *Biomedicine & Pharmacotherapy*, no. 109, pp. 1249-1258, 2019. https://doi.org/10.1016/j.biopha.2018.10.078.

43. William A. C., Barry B. W. "Penetration Enhancers." *Adv. Drug Deliv. Rev.*, no. 56, pp. 603-618, 2004. https://doi.org/10.1016/j.addr.2003.10.025.

44. X. Hong, L. Wei, F. Wu, Z. Wu, L. Chen, Z. Liu, W. Yuan. "Dissolving and Biodegradable Microneedle Technologies for Transdermal Sustained Delivery of Drug and Vaccine" *Drug Des. Devel. Ther.*, no. 7, pp. 945-952, 2013.

45. Sur S., *et al.* "Remote Loading of Preen-capsulated Drugs into Stealth Liposomes." *Proceedings of the National Academy of Sciences of the United States of America*, no. 111, pp. 2283-2288, 2014. doi:10.1073/pnas.1324135111.

46. Akbarzadeh A., *et al.* "Liposome: Classification, Preparation, and Applications*." Nanoscale research letters*, no. 8, 2013. doi:10.1186/1556-276X-8-102.

47. Avcil M., *et al*. "Microneedles in Drug Delivery: Progress and Challenges." *Micromachines (Basel)*, no. 12, vol. 11, pp. 1321, 2021. doi:10.3390/mi12111321.

48. Resnik D., *et al*. "In Vivo Experimental Study of Noninvasive Insulin Microinjection through Hollow Si Microneedle Array." *Micromachines* vol. 9, no. 1, pp. 40, 2018, doi:10.3390/mi9010040.